Electronic Supplementary Information

Aggregation-induced emission triggered by the radiative-transition-switch of a cyclometallated Pt(II) complex

Yuanhui Sun,[a] Xiaolong Yang,[a] Boao Liu,[a] Haoran Guo,[a] Guijiang Zhou,[*a] Wei Ma[*b] and Zhaoxin Wu[*c]

[a] MOE Key Laboratory for Nonequilibrium Synthesis and Modulation of Condensed Matter, Department of Chemistry, School of Science, Xi'an Jiaotong University, Xi'an 710049, China. E-mail: zhougj@mail.xjtu.edu.cn

[b] State Key Laboratory for Mechanical Behavior of Materials, Xi'an Jiaotong University, Xi'an 710049, China. E-mail: msewma@xjtu.edu.cn

[c] Key Laboratory of Photonics Technology for Information, School of Electronic and Information Engineering, Xi'an Jiaotong University, China. E-mail: zhaoxinwu@mail.xjtu.edu.cn

Table of Contents

General information

The commercially available starting materials were used directly without further purification. All reactions were performed under a nitrogen atmosphere. ^{1}H, and ^{13}C NMR spectra were recorded on a Bruker Avance 400 MHz spectrometer in $CDCl_3$ solutions with chemical shifts referenced to the solvent residual peak. Mass spectral (MS) measurements were measured on a WATERS I-Class VION IMS QTof mass spectroscopy. The thermalgravimetric analysis (TGA) data was measured on a NETZSCH STA 409C instrument. UV-vis absorption spectrum was measured on a Shimadzu UV-2250 spectrophotometer in CH_2Cl_2 at room temperature. Photoluminescence spectra and lifetimes were measured on an Edinburgh Instruments Ltd (FLS920) fluorescence spectrophotometer. The photoluminescence quantum yield (PLQY) in solution was determined against *fac*-[Ir(ppy)$_3$] standard (PLQY = 0.97) at room temperature.[1] The PLQY of **DPA-Pt** neat film was tested with an integrating sphere installed on the FLS920 fluorescence spectrophotometer. The cyclic voltammetry measurement was conducted on a Princeton Applied Research (PARSTAT 2273, Advanced Electrochemical System) equipment in CH_3CN solutions containing *n*-Bu_4NPF_6 as the supporting electrolyte at a scan rate of 100 mV s^{-1}. Ferrocene/ferrocenium (Fc/Fc^+) was used as the internal reference. The HOMO and LUMO energy levels were calculated using the first oxidation peak potential (E_{ox}) and reduction peak potential (E_{red}) according to the equations $E_{HOMO} = -(E_{ox} + 4.8)$ eV and $E_{LUMO} = -(E_{red} + 4.8)$ eV.

X-ray Crystallography. Single crystal of **DPA-Pt** was formed from the THF/hexane solution by slow evaporation of the solvent. The crystal data were collected on a Bruker SMART CCD diffractometer (Mo Kα radiation and λ = 0.71073 Å) in Φ and ω scan modes at ca. 293 K. The

structure was solved by direct methods followed by difference Fourier syntheses, and then refined by full-matrix least-squares techniques against F^2 using SHELXL-97[2] program on a personal computer.

Theoretical Computation. Geometrical optimizations were conducted using the popular B3LYP functional theory. The basis set used for C, H, O, and N atoms was 6-31G (d, p). The basis set used for Pt atom was LanL2DZ. The energies of the excited states of the complex were computed by time-dependent DFT (TD-DFT) based on optimized geometry at the ground state. The natural transition orbitals (NTOs) were calculated based on the optimized T_1 geometry. All calculations were carried out by using the Gaussian 09 program.[3]

GIWAXS measurement. GIWAXS measurement was performed at beamline 7.3.3 at the Advanced Light Source. Samples were prepared on Si substrates by vacuum deposition. The 10 keV X-ray beam was incident at a grazing angle of 0.13°−0.17°, which maximized the scattering intensity from the samples. The scattered X-rays were detected using a Dectris Pilatus 2M photon counting detector.

OLED Fabrication and Measurements. The devices were fabricated by vacuum-deposition method under a pressure around 10^{-3} Pa. The ITO glass substrates were pre-cleaned with acetone and deionized water, and then exposed to ultraviolet-ozone for *ca.* 1 min. Then, the functional layers were deposited. The thickness of each layer was monitored by a quartz thickness monitor. The emissive layer of device A was 6 wt% **DPA-Pt** doped CBP film. The emissive layer of device B was vacuum-deposited **DPA-Pt** neat film. The brightness–voltage curves of the resultant devices were recorded with a Keithley 2602 and Source Meter. The EL spectral were recorded with a PR650 SpectraScan spectrometer. The efficiency and spectral measurements were carried out under ambient

conditions.

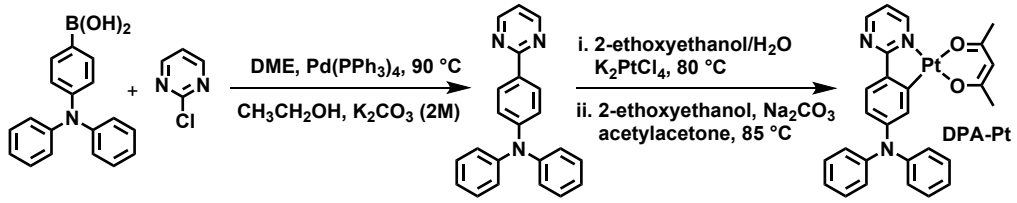

Scheme S1. Synthesis of **DPA-Pt**.

Synthesis of *N,N*-diphenyl-4-(pyrimidin-2-yl)aniline: Under a nitrogen atmosphere, boronic acid compounds (1.05 g, 3.6 mmol), 2-chloropyrimidine (0.38 g, 3.3 mmol), and $Pd(PPh_3)_4$ (0.19 g, 0.16 mmol) were dissolved in a mixture of 1,2-dimethoxyethane (DME, 25 mL), ethanol (5 mL) and K_2CO_3 solution (2M, 20 mL). After heated to 90 °C and stirred overnight, the mixture was allowed to cool to room temperature and then was extracted with CH_2Cl_2 several times. The combined organic layers were dried over anhydrous Mg_2SO_4. After the removal of solvent, the residual was purified on a silica column using a mixture of petroleum ether and CH_2Cl_2 as the eluent to give the organic ligand *N,N*-diphenyl-4-(pyrimidin-2-yl)aniline as pale yellow solid (0.85 g, yield: 80.5 %). ^{1}H NMR (400 MHz, $CDCl_3$, δ): 8.75 (d, J = 4.8 Hz, 2H), 8.28 (d, J = 8.8 Hz, 2H), 7.29 (t, J = 8.0 Hz, 4H), 7.17–7.09 (m, 9H); ^{13}C NMR (100 MHz, $CDCl_3$, δ): 164.49, 157.12, 150.27, 147.22, 130.81, 129.36, 129.14, 125.16, 123.60, 122.06, 118.22.

Synthesis of DPA-Pt: Under a nitrogen atmosphere, the pyrimidine-based ligand (0.37 g, 1.1 mmol) and K_2PtCl_4 (0.41 g, 1.0 mmol) were added to a mixture of 2-ethoxyethanol and water (3:1, v/v, 35 mL). After stirred at 80 °C for *ca.* 6 h, the reaction mixture was cooled to room temperature. Water (30 mL) was added and colored precipitate was formed. The precipitate was filtered, dried, and used without further purification in the following step. Under a nitrogen atmosphere, the precipitate, Na_2CO_3 (1.06 g, 10 mmol), and acetylacetone (0.5 g, 5 mmol) were added to 2-

ethoxyethenol (30 mL). After stirred at 85 °C for *ca.* 12 h, the reaction mixture was cooled to room temperature. Then, water (30 mL) was added and colored precipitate was formed. The precipitate was filtered, dried, and purified on preparative TLC plates using a mixture of petroleum ether and CH_2Cl_2 as the eluent to obtain **DPA-Pt** as yellow powder (0.20 g, yield: 32.5%). MS: m/z 616. ^{1}H NMR (400 MHz, $CDCl_3$, δ): 8.98 (d, J = 5.6 Hz, 1H), 8.68 (t, J = 2.0 Hz, 1H), 7.61 (d, J = 8.8 Hz, 1H), 7.31–7.26 (m, 4H), 7.22–7.18 (m, 5H), 7.08 (t, J = 7.2 Hz, 2H), 6.91 (t, J = 5.2 Hz, 1H), 6.78 (d, J = 8.4 Hz, 1H), 5.39 (s, 1H), 1.95 (s, 3H), 1.72 (s, 3H); ^{13}C NMR (100 MHz, $CDCl_3$, δ): 185.72, 184.10, 175.79, 157.80, 153.61, 150.40, 147.13, 139.30, 133.52, 129.18, 127.71, 126.00, 123.71, 121.13, 116.98, 115.18, 102.37, 28.17, 26.74.

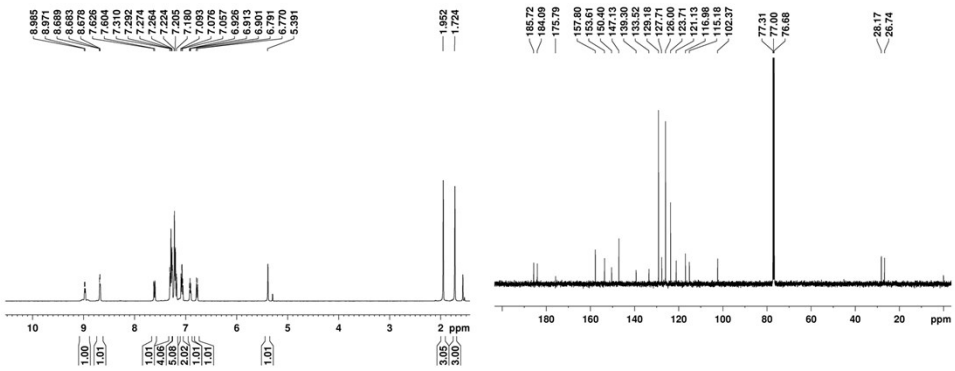

Fig. S1 The ^{1}H and ^{13}C NMR spectra of **DPA-Pt**.

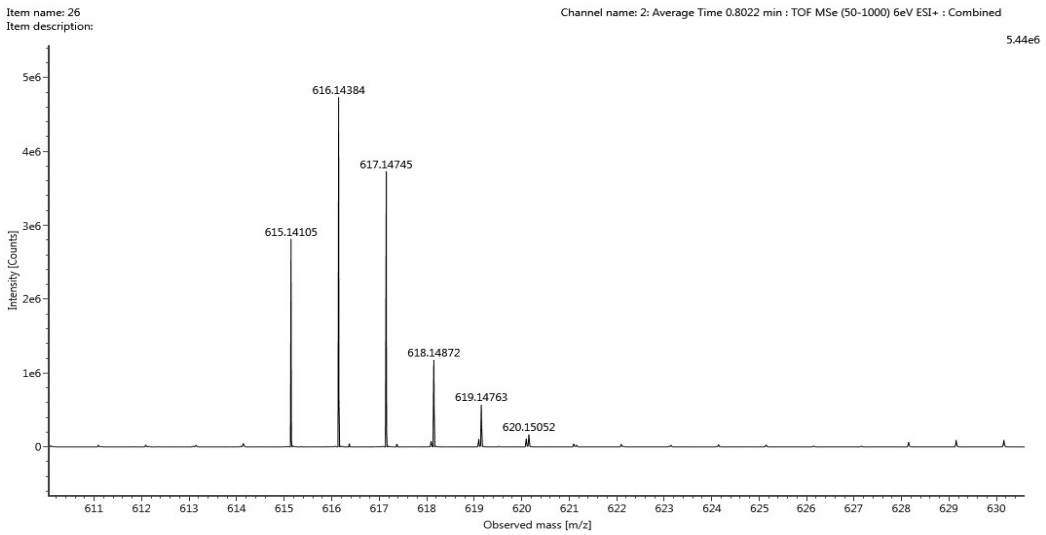

Fig. S2 The MS spectrum of **DPA-Pt**.

Table S1 Crystal data and structure refinement details

Complex	**DPA-Pt**
CCDC	1504806
formula	$C_{27}H_{23}N_3O_2Pt$
M (g mol^{-1})	616.57
crystal system	Triclinic
space group	P-1
a (Å)	9.0445(13)
b (Å)	10.5520(15)
c (Å)	13.010(2)
α (°)	81.909(9)
β (°)	70.755(9)
γ (°)	84.493(9)
V (Å^3)	1159.0(3)
Z	2
D_{calcd} (g cm^{-3})	1.767
μ (mm^{-1})	6.083
F(000)	600
θ range (°)	1.67 to 24.79
reflections collected	12146
independent reflections	3885
R_{int}	0.0297
R ($I > 2\sigma(I)$)	R1 = 0.0235, wR2 = 0.0552
R (all data)	R1 = 0.0314, wR2 = 0.0590

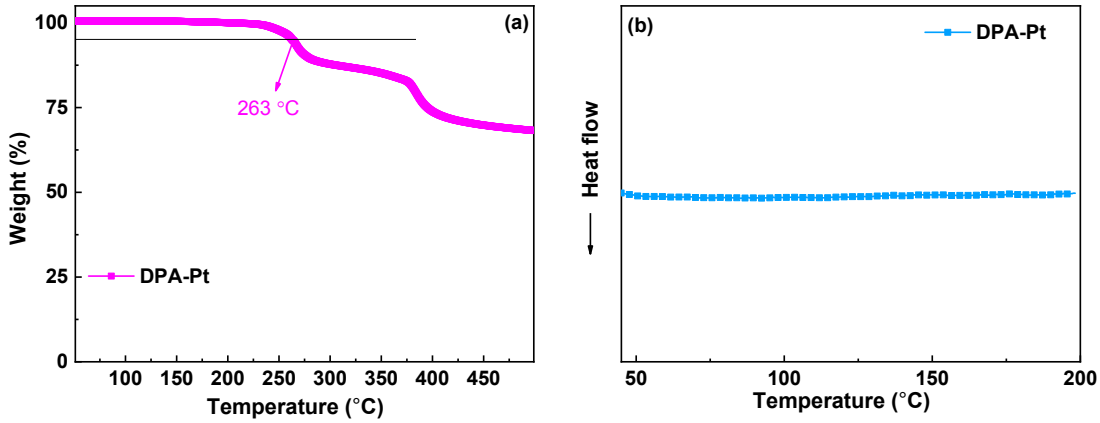

Fig. S3 (a) TGA and (b) DSC curves of **DPA-Pt**.

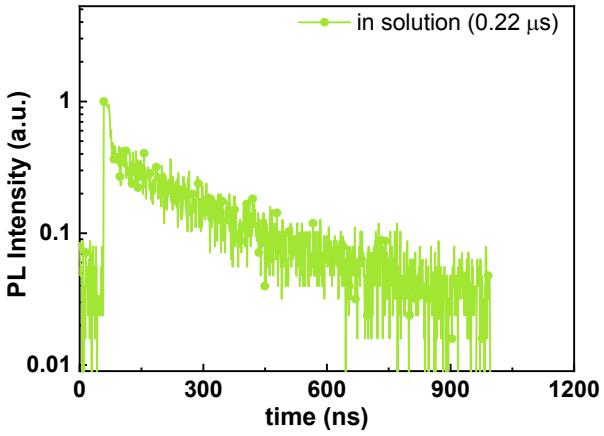

Fig. S4 The lifetime decay profile of the phosphorescence emission band of **DPA-Pt** in solution.

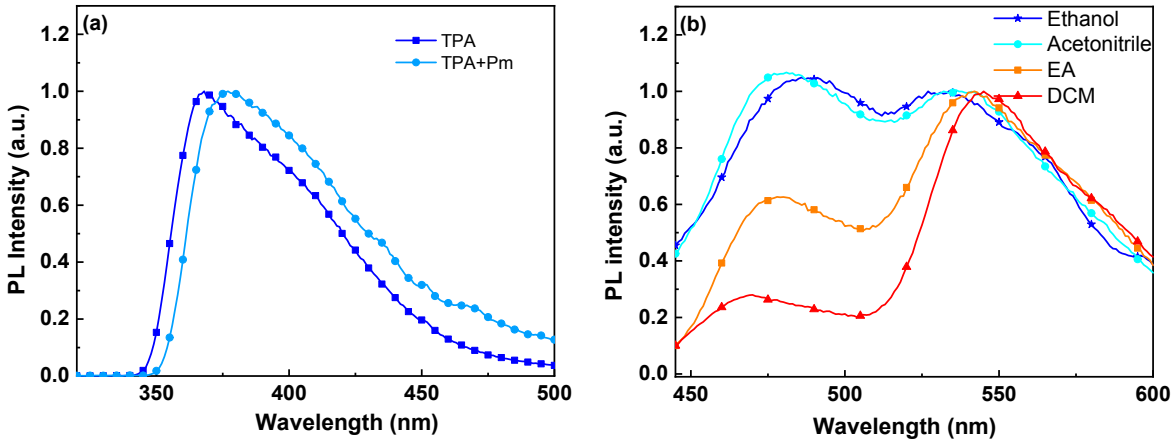

Fig. S5 (a) PL spectra of triphenylamine (TPA) and the mixture (TPA+Pm) of pyrimidine moiety and TPA in dichloromethane (DCM) ; (b) PL spectra of **DPA-Pt** in ethanol, acetonitrile, ethyl acetate (EA), and DCM at r.t.

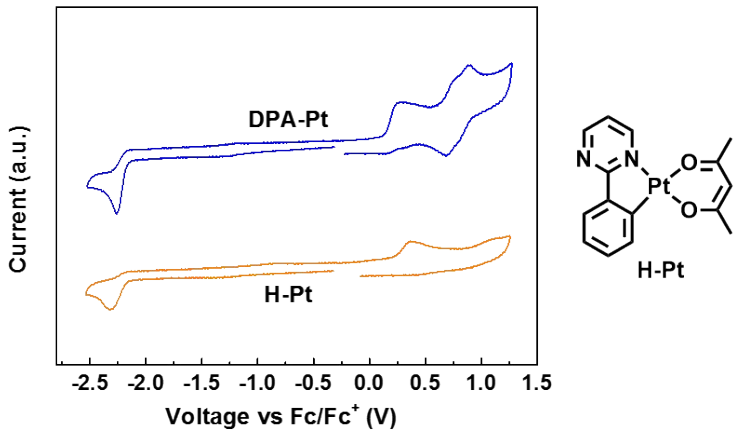

Fig. S6 Cyclic voltammetry curves of **DMA-Pt** and **H-Pt**.

Table S2 DTF and TD-DFT results for **DPA-Pt** based on the optimized S_0 geometries [a]

Complex	MOs	Contribution from metal centre orbitals and ligand orbitals to MOs (%)				Energy levels (eV)	Main contribution for $S_0 \rightarrow S_1$ excitation/E_{cal}/f	Main contribution for $S_0 \rightarrow T_1$ excitation/E_{cal}
DPA-Pt		**Pt**	**Cyc-L**	**DPA**	acac			
	L+1	0.65	96.21	2.97	3.14	−1.39	H → L (90.7%)	H → L (76.8%)
	L	6.19	92.25	4.37	1.56	−1.68	449 nm	H → L+1 (12.6%)
	H	1.05	98.69	63.31	0.26	−4.88	0.1721	552 nm

[a] H and L stand for HOMO and LUMO, respectively. **Cyc-L** is the pyrimidine-based cyclometalating ligand. **DPA** is *N,N*-diphenylamino moiety. Acac is acetylacetone ligand. E_{cal} and f are the calculated excitation energy in wavelength and oscillator strength, respectively.

Table S3 NTO results for **DPA-Pt** based on the optimized T_1 geometries [a]

Complex	NTOs	Contribution from metal centre orbitals and ligand orbitals to NTOs (%)			
DPA-Pt		**Pt**	**Cyc-L**	**DPA**	acac
	Particle	4.64	94.65	8.90	0.71
	Hole	3.72	95.87	34.54	0.41

[a] **Cyc-L** is the pyrimidine-based cyclometalating ligand. **DPA** is the *N,N*-diphenylamino moiety. Acac is acetylacetone ligand.

Table S4 NTO results for **DMA-Pt** dimer based on the optimized T_1 geometry [a]

Complex	NTOs	Contribution from metal centre orbitals and ligand orbitals to NTOs (%)			
DPA-Pt		**Pt1/Pt2**	**Cyc-L1/Cyc-L2**	**Py1/Py2**	acac1/acac2
	Particle	5.51/5.51	43.38/43.40	32.84/32.86	1.10/1.10
	Hole	41.88/41.88	5.00/5.00	1.77/1.77	3.12/3.12

[a] **Pt1/Pt2** are the two Pt centers in the dimer. **Cyc-L1/Cyc-L2** are the two pyrimidine-based cyclometalating ligands. **Py1/Py2** are the two pyrimidine rings. Acac1/acac2 are the two acetylacetone ligands.

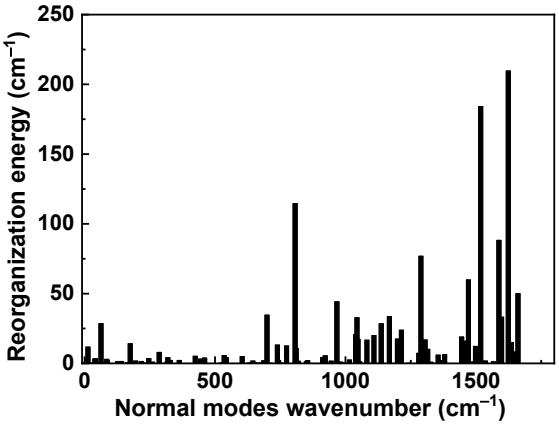

Fig. S7 The calculated reorganization energy versus the normal mode wave numbers.

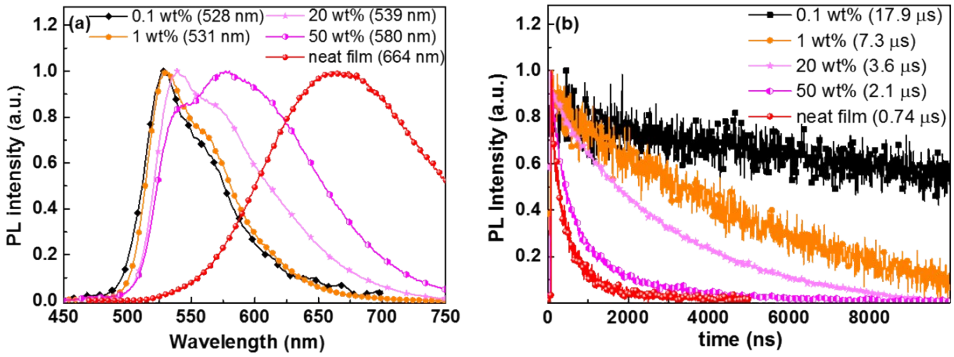

Fig. S8 (a) PL spectral of PMMA films doped with **DPA-Pt** at different doping levels. (b) Transient PL decay spectra of PMMA films doped with **DPA-Pt** at different doping levels. (Neat film was prepared by the vacuum-deposition method.)

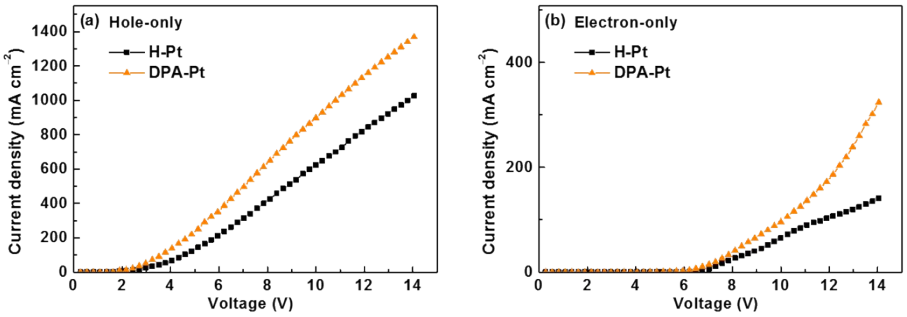

Fig. S9 The *J*–*V* curves of (a) hole-only and (b) electron-only devices.

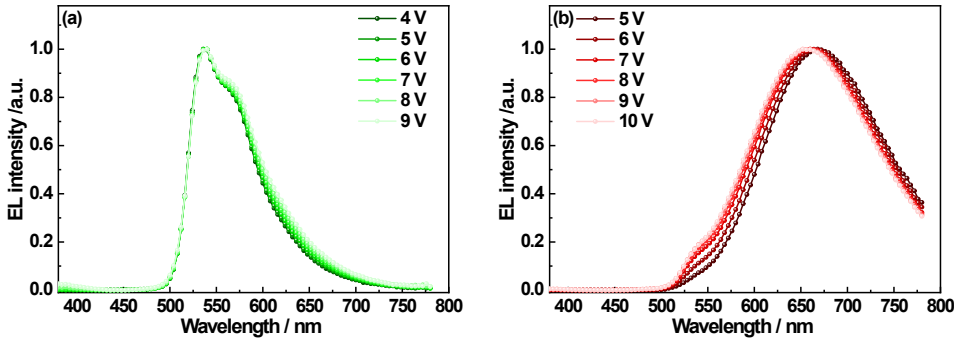

Fig. S10 The EL spectra of devices at various driving voltages.

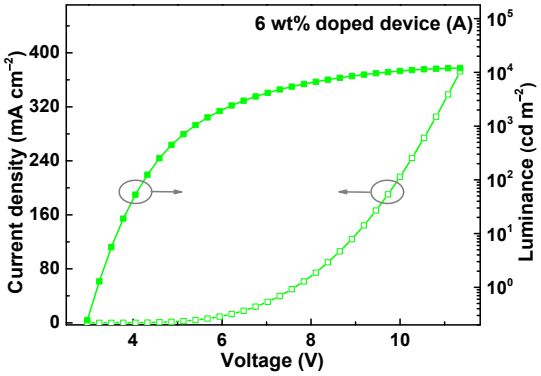

Fig. S11 *J*–*V*–*L* characteristics of device A.

References

1 T. Sajoto, P. I. Djurovich, A. B. Tamayo, J. Oxgaard, W. A. Goddard and M. E. Thompson, *J. Am. Chem. Soc.*, 2009, **131**, 9813-9822.

2 G. M. Sheldrick, SHELXL-97: Program for Crystal Structure Refinement; University of Göttingen: Göttingen, Germany, 1997.

3 M. J. Frisch, G. W. Trucks, H. B. Schlegel, G. E. Scuseria, M. A. Robb, J. R. Cheeseman, G. Scalmani, V. Barone, B. Mennucci, G. A. Petersson, H. Nakatsuji, M. Caricato, X. Li, H. P. Hratchian, A. F. Izmaylov, J. Bloino, G. Zheng, J. L. Sonnenberg, M. Hada, M. Ehara, K. Toyota, R. Fukuda, J. Hasegawa, M. Ishida, T. Nakajima, Y. Honda, O. Kitao, H. Nakai, T. Vreven, J. A. Montgomery, J. E. P. Jr., F. Ogliaro, M. Bearpark, J. J. Heyd, E. Brothers, K. N. Kudin, V. N. Staroverov, R. Kobayashi, J. Normand, K. Raghavachari, A. Rendell, J. C. Burant, S. S. Iyengar, J. Tomasi, M. Cossi, N. Rega, J. M. Millam, M. Klene, J. E. Knox, J. B. Cross, V. Bakken, C. Adamo, J. Jaramillo, R. Gomperts, R. E. Stratmann, O. Yazyev, A. J. Austin, R. Cammi, C. Pomelli, J. W. Ochterski, R. L. Martin, K. Morokuma, V. G. Zakrzewski, G. A. Voth, P. Salvador, J. J. Dannenberg, S. Dapprich, A. D. Daniels, Ö. Farkas, J. B. Foresman, J. V. Ortiz, J. Cioslowski and D. J. Fox. *Gaussian 09, Revision A.01*, Gaussian, Inc.: Wallingford CT, 2009.